Water Science and Engineering, 2009, 2(4): 60-68
doi:10.3882/j.issn.1674-2370.2009.04.006

http://kkb.hhu.edu.cn
e-mail: wse@hhu.edu.cn

Experimental study on dynamic pipe fracture in consideration of hydropower plant model

Kazumi ISHIKAWA*, Yukio KONO, Akira HAGA, Kazuo KATO, Kota SUGAWARA

College of Engineering, Tohoku Gakuin University, Miyagi 985-8537, Japan

Abstract: In the case of sudden valve closure, water hammer creates the most powerful pressure and damage to pipeline systems. The best way to protect the pipeline system is to eliminate water hammer. The main reasons for water hammer occurrence are valve closure, high initial velocity, and static pressure. However, it is difficult to eliminate water hammer. Water hammer tends to occur when the valve is being closed. In this study, the pipe fracture caused by static water pressure, gradually increasing pressure, and suddenly increasing pressure were compared experimentally in a breaking PVC test pipe. The quasi-static zone, the dynamic zone, and the transition zone are defined through the results of those experiments, with consideration of the fracture patterns of test pipes and impulses. The maximum pressure results were used to design the pipeline even though it is in the dynamic zone.

Key words: *hydropower plant; dynamic pipe fracture; pipeline; impulse; water hammer*

1 Introduction

In pipeline systems, there are three cases of pipeline breakage that are caused by high pressure from inside of the pipeline. The first is high static pressure. The second is water hammer caused by sudden valve closure. The third is high pressure that increases gradually (water hammer), caused by gradual valve closure. In almost all cases in which engineers come across trouble, two or three of these conditions are occurring simultaneously. In the case of sudden valve closure, water hammer creates the most powerful pressure and damage to pipeline systems (Watters 1979; Wylie and Streeter 1978; Kono and Watanabe 2002; Kono et al. 2005; Ishikawa et al. 2008).

The best way to protect the pipeline system is to eliminate water hammer. The main reasons for water hammer occurrence are valve closure, high initial velocity, and static pressure. However, it is difficult to eliminate water hammer. Water hammer tends to occur when the valve is being closed (Kono et al. 1998), as in a major accident at a hydropower plant in Russia on August 17, 2009. It is very difficult to investigate the cause of the accident when the accident actually occurs. The large water hammer in water pipelines could be one of the causes of pipeline accidents because the water hammer creates the most powerful pressure

*Corresponding author (e-mail: *ishikawa@tjcc.tohoku-gakuin.ac.jp*)
Received Sep. 29, 2009; accepted Nov. 17, 2009

inside the pipes.

In this study, pipe fractures caused by static water pressure, gradually increasing pressure, and suddenly increasing pressure were compared experimentally in a breaking PVC test pipe. The quasi-static zone, the dynamic zone, and the transition zone are defined through the results of those experiments, with consideration of the fracture patterns of test pipes and impulses. The maximum pressure results were used to design the pipeline even though it is in the dynamic zone.

2 Hydropower plant model and power generation

Fig. 1 shows the hydropower plant model for the experiment. Power generation (kW) is

$$P_0 = 9.8QH\eta \tag{1}$$

where Q is the water quantity (m^3/s), H is the effective head (m), and η is the total efficiency. When the inside diameter of the water pipe is D (m), the cross section area is S (m^2), and the average velocity of the cross section is u (m/s), Eq. (1) changes to Eq. (2):

$$P_0 = 9.8SuH\eta \tag{2}$$

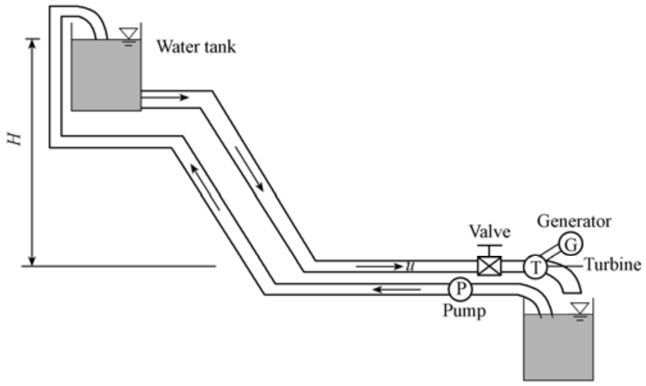

Fig. 1 Hydropower plant model

In Fig. 1, the water tank contains 4.5 m^3 of water, the effective head is 12 m, and the inside diameter of the water pipe is 53.4 mm. When the average velocity of the cross section is 1.0 m/s and total efficiency is 0.84, power generation is equal to 0.221 kW.

For example, a large hydropower plant of the neighboring prefecture has four generators and four turbines. The specifications are a water quantity of 78.5 m^3/s, an effective head of 387 m, an inside diameter of the water pipe of 3.16 m, an average velocity of the cross section of 10 m/s, and a total efficiency of 0.84. Each generator can generate the electric power of 2.5×10^5 kW. Total generator generates 1.0×10^6 kW of maximum electric power.

Fig. 2 shows the characteristics of pressure in the hydropower plant model when the average velocity of the cross section is 0.893 m/s. The maximum pressure value in Fig. 2 is about 1.0 MPa.

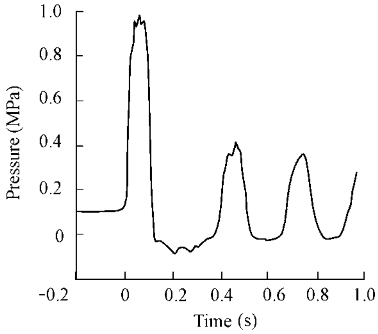

Fig. 2 Characteristics of pressure in hydropower plant model

3 Experiment of pipe fracture under water pressure

3.1 Method of experiment

The PVC test pipe was 388 mm in total length and 56 mm in diameter, and two sockets were glued to the ends to connect with the experimental apparatus as shown in Fig. 3. The central part of the test pipe was 100 mm in length (*L*) and 0.4 mm in thickness (*e*). Fig. 4 is a diagram of the experimental apparatus. The stabilizer was attached between a water pump and the test pipe to smooth the pressure loading on the pipe from the pump. The test pipe was fixed with four steel plates so as not to expand longitudinally or to be loaded with eccentric forces. Two pressure transducers (PT-1 and PT-2) were placed, one at each side of the pipe. The pressure acting on the test pipe was taken by the two pressure transducers, amplified by the strain meter, and sent to a computer. Two high-speed video cameras recorded the fracture of test pipes every 1/2 000 seconds. These electrical devices were simultaneously controlled by a computer. The PVC test pipes were used one hundred times each year, and the study began about ten years ago.

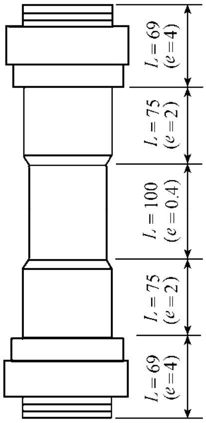

Fig. 3 PVC test pipe (Unit: mm)

The water pressure loading time was controlled by inflow, and the flow rate was controlled by the valve, which is attached in front of the pump. The loading time was set from one second to nine minutes and the water pressure was increased quickly or gradually until the test pipe broke (Atkins and Mai 1985).

The pressure data were accepted only if there was no leakage and no eccentric force, and they were synchronized with the high-speed cameras. The breakage patterns, the direction of crack initiation, the flight length of broken pieces, and the length of water splashing were measured simultaneously.

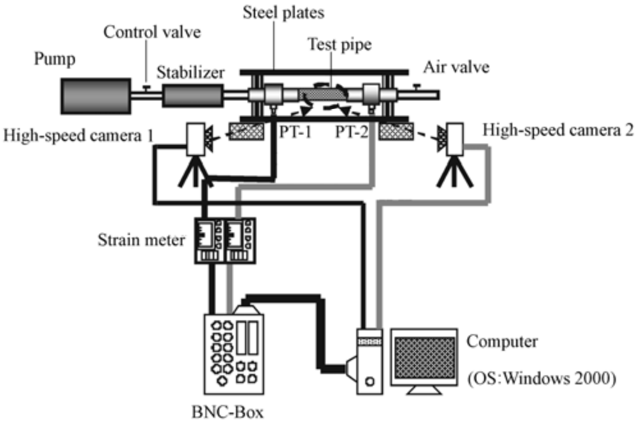

Fig. 4 Experimental apparatus

3.2 Results

Fig. 5 shows the pressure patterns acting on the test pipes. The maximum pressure does not occur just before the pipe breakage because of the creep phenomenon of the test pipe. The test pipe is swollen in circumferential directions and the pressure drops because of expansion of the area. For this reason, the maximum pressure was used as the strength of the pipe material even though the pressure just before the breakage of the pipe was lower than the maximum pressure.

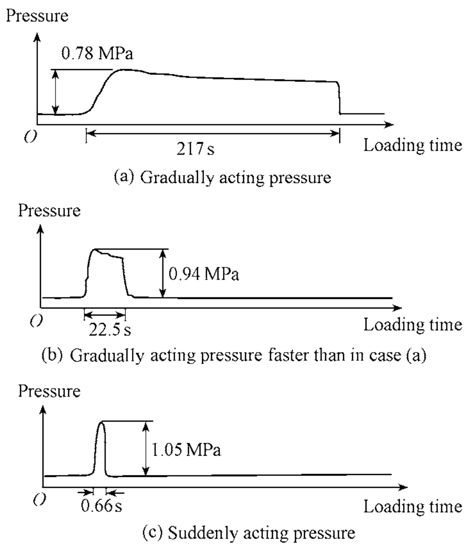

Fig. 5 Pressure histories

Fig. 6 is an illustration of the breakage patterns of the test pipe. When the pressure acts on the test pipe very slowly (Fig. 6(a)), the pipe swells gradually and becomes a balloon. Finally, it breaks completely. When the pressure on the test pipe gradually rises (Fig. 6(b)), a little faster than in the case of Fig. 6(a), the pipe swells, and a thin and weak line develops in the longitudinal direction. Finally, a small hole appears on the line, water leaks out from this hole, and the pressure drops. When the pressure acting on the test pipe rises a little faster than in the case of Fig. 6(b) (Fig. 6(c)), the test pipe swells first, then the pressure acts on the pinhole, and the crack initiates and opens suddenly from the inside due to the extra pressure. The test pipe swells and breaks in an “x” pattern. Small cracks occur simultaneously on both sides of the “x”. When the pressure acts on the test pipe quickly (Fig. 6(d)), the pipe breaks suddenly in an “x” pattern without swelling.

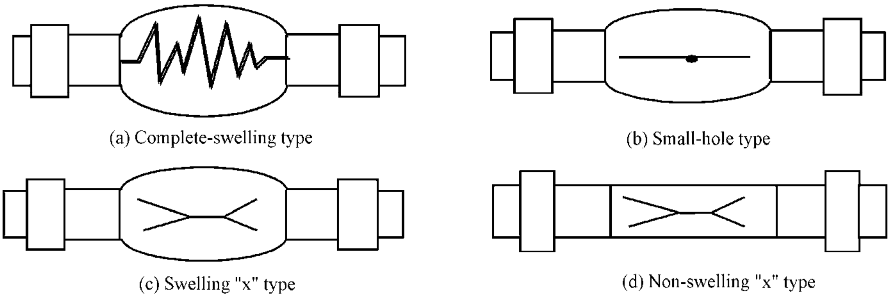

Fig. 6 Breakage patterns

3.3 Classification of fracture zones by breakage patterns

The maximum pressure (P) versus loading time (t) results are shown in Fig. 7. Fig. 8 shows the dynamic zone, the quasi-static zone, and the transition zone. The linear equation of least squares is $P = -0.003\,7t + 1.04$ in less than 43.7 s of loading time. This area is classified as the dynamic loading zone. The linear equation of least squares is $P = -0.000\,088t + 0.88$ between 43.7 s and 777.8 s of loading time. This area is classified as the transition zone. The maximum pressure exceeding 777.8 s of loading time is 0.81 MPa, according to least square analysis in the transition zone. This area is classified as the quasi-static zone. These experimental results were compared with the results of the impulse data (Kono et al. 1995). The maximum pressure increases to 0.88 MPa at the boundary between the transition zone and the dynamic zone, at 43.7 s of loading time. The maximum pressure becomes 1.04 MPa when the loading time is equal to zero.

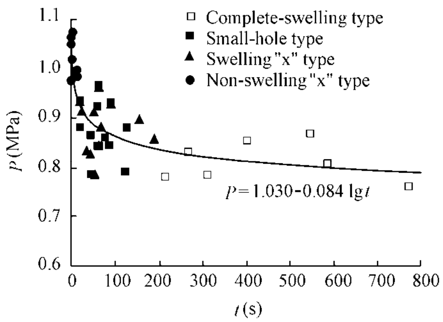

Fig. 7 Maximum pressure vs. loading time

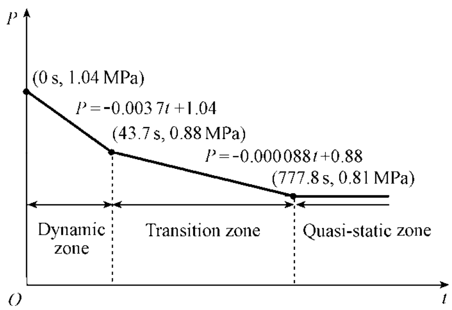

Fig. 8 Classification of dynamic zone, transition zone and quasi-static zone

3.4 Dynamic characteristics of pipe material

The test piece for the dynamic tensile experiment is shown in Fig. 9. The test pieces with sizes of 10 mm × 50 mm × 2 mm were cut from PVC pipes. There were five tensile test speeds V: 0.2, 2.0, 20.0, 200.0, and 1 000.0 mm/min. The dynamic tensile tests were carried out three times at each test speed. Fig. 10 shows the dynamic stress-strain curves. It can be seen from Fig. 10 that the dynamic strength of the PVC test pieces increased with test speed as follows: 42 MPa at a test speed of 0.2 mm/min, 48 MPa at a test speed of 2.0 mm/min, 51 MPa at a test speed of 20.0 mm/min, 58 MPa at a test speed of 200.0 mm/min, and 62 MPa at a test speed of 1000.0 mm/min. The maximum pressure increased with the reduction of the loading time in the dynamic zone as shown in Fig. 8. The maximum pressure can be used to calculate the thickness of the pipes for each dynamic loading time. The strength of the pipes also increased with test speed, which is the same as shortening the loading time. The dynamic maximum pressure can be used to design the thickness of pipes. However, the dynamic design method has a limitation, because the acceleration term increases. The result of the tensile test at the test speed of 1000.0 mm/min was a strength of 62 MPa, a pressure of 0.89 MPa, and 25 s of loading time. This was within the dynamic zone. The result of the tensile test at a test speed of 200.0 mm/min was a strength of 58 MPa, a pressure of 0.83 MPa, and 300 s of loading time. This was within the transition zone. The results at the test speed less than 20 mm/min were within the quasi-static zone (Narisawa 1982; Greenshields and Leevers 2000).

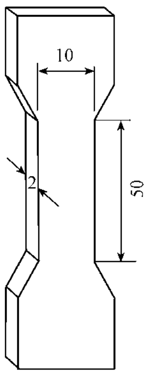

Fig. 9 Test piece of PVC pipe (Unit: mm)

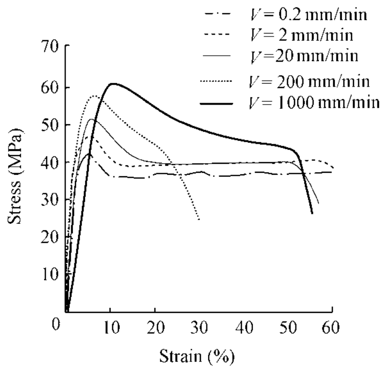

Fig. 10 Dynamic stress-strain curves

3.5 Classification of fracture zones by impulse

In the quasi-static zone, the values of impulse (*Y*) are large when the loading time is long, even though the maximum pressure is low. On the other hand, in the dynamic zone, the impulse is small when the loading time is short, even though the maximum pressure is high. The impulse is shown in Fig. 11 as a function of loading time. We let the slope change two times. The changing point at a loading time of 515.9 s was between the quasi-static zone and the transition zone. The changing point at a loading time of 27.38 s was between the dynamic zone and the transition zone. A change in the slope means that the characteristics of the fracture change. The classification of zone by impulse resembles classification by breakage pattern. The impulse approaches zero when the loading time is decreasing, even though the maximum pressure is rising. The result for the water hammer impulse was higher than the extension of the regression line of the dynamic zone shown in Fig. 12. This means that there is a zone other than the dynamic zone in this area. The boundary for the quasi-static zone is between 515.9 s and 777.8 s of loading time.

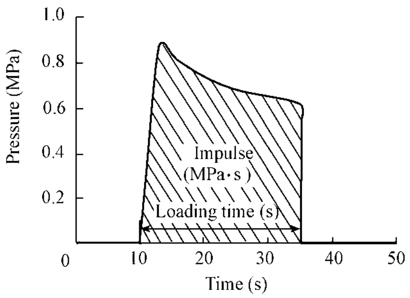

Fig.11 Impulse of pipe fracture

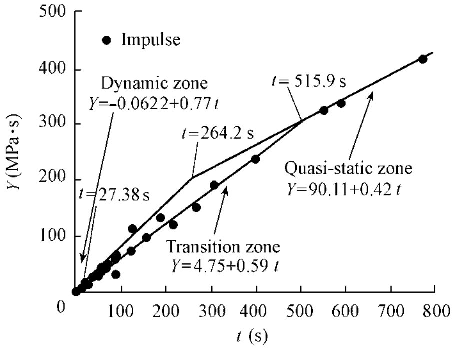

Fig. 12 Classification of fracture zones by impulse

4 Theoretical analysis

The equation for radial motion in cylindrical coordinates is

$$\frac{\partial \sigma_r}{\partial r} + \frac{\sigma_r - \sigma_\theta}{r} = \rho \frac{\partial v}{\partial t} \tag{3}$$

where ρ is the density of water, r is the radius of the pipe, σ_θ is the stress in the circumferential direction, σ_r is the stress in the radial direction, and v is the speed of pipe expansion in the radial direction.

Eq. (3) becomes Eq. (4) by integration from r_0 to r and 0 to ε_θ:

$$2\pi \int_{r_0}^{r} pr\mathrm{d}r = 2\pi r_0 h_0 \int_0^{\varepsilon_\theta} \sigma_\theta \mathrm{d}\varepsilon_\theta + \pi \rho r_0 h_0 v^2 \tag{4}$$

where h_0 is the thickness of the pipe; p is the pressure: $p = \sigma_r$; ε_θ is the strain in the circumferential direction: $\varepsilon_\theta = \frac{\mathrm{d}r}{r}$; h_0 is the initial thickness; and r_0 is the initial radius.

The energy equation is as follows:

$$W_\mathrm{e} = W_\mathrm{p} + W_\mathrm{k} \tag{5}$$

where W_e is the work done by the inner pressure per unit length of pipe, W_p is the work done by elastic-plastic deformation of pipe material, and W_k is the kinetic work. This equation shows that the work done by the inner pressure can be separated into the work done by the circumferential elastic-plastic work and that done by the kinetic work.

The kinetic work increases with the square of the speed of pipe expansion in the radial direction as the loading time approaches zero, as shown in Fig. 13. However, the work done by elastic-plastic deformation of the pipe converges to a certain value, because it is assumed that the maximum stress of the dynamic tensile test converges with increasing tensile speed.

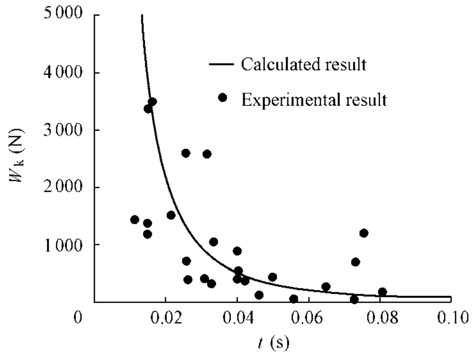

Fig. 13 Kinetic work vs. loading time

5 Conclusions

As a result of this study, the loading and breaking regions were classified into three zones: the quasi-static zone, the dynamic zone, and the transition zone.

The dynamic strength of PVC pieces in tensile tests was as follows: 42 MPa at a test speed of 0.2 mm/min, 48 MPa at a test speed of 2.0 mm/min, 51 MPa at a test speed of 20.0 mm/min, 58 MPa at a test speed of 200.0 mm/min, and 62 MPa at a test speed of 1 000.0 mm/min. The dynamic stress-strain curve of PVC pipes shows that the strength of PVC test pieces increases with test speed. However, the experimental results show that the maximum stress of a dynamic tensile test converges with the increase of tensile speed.

The experimental results show that the average breaking pressure is 0.81 MPa in the quasi-static zone. The boundary of the quasi-static zone is between 515.9 s and 777.8 s of loading time. The maximum pressure increases to 0.88 MPa at the boundary between the transition zone and the dynamic zone, at 43.7 s of loading time.

The loading time of the dynamic zone is less than 43.7 s according to the observed breakage pattern, and less than 27.38 s according to the impulse, when the dynamic characteristics of pipe materials are taken into consideration. The maximum pressure becomes 1.04 MPa when the loading time is equal to zero.

The steel pipeline of the hydropower plant model is about 60 m long. A PVC test pipe with a length of 0.388 m was used to investigate pipe breakage in this study. It could be applied to other materials, such as steel, copper and aluminum, by using Eq. (3) and changing the parameters of pipe materials.

In the quasi-static zones, the pipeline can generally be designed based on the strength of its material and the pressure acting on it. In the dynamic zone and the transition zone, the pipeline can be designed using the dynamic maximum pressure at the loading time. The pipeline cannot be protected by the usual design, as the thickness of pipes increases, because the influence of the radial inertia becomes greater in comparison with the work done by elastic-plastic deformation of pipe materials. These results are very important to the design of hydropower plant pipelines.

References

Atkins, A. G., and Mai, Y. W. 1985. *Elastic and Plastic Fracture: Metals, Polymers, Ceramics, Composites, Biological Materials*. Chichester: Ellis Horwood Ltd.

Greenshields, C. J., and Leevers, P. S. 2000. Failure of plastic water pipes by surge and cavitation. *Proceedings of the 8th International Conference on Pressure Surges*, 377-391. The Hague: BHRGroup.

Ishikawa, K., Kono, Y., Haga, A., and Kato, K. 2008. Dynamic pipe fracture in water pipeline. *Proceedings of the 16th IAHR- APD Congress and 3rd Symposium of IAHR- ISHS, Volume VI: Hydropower Hydraulics*, 2134-2139. Bejing: Tsinghua University Press.

Kono, Y., Sugano, T., and Watanabe, M. 1995. Experimental study on dynamic fracture of pipes by water hammer and quasi-static fracture by water pressure. *Japan Society of Civil Engineers*, 509/II-30, 55-65. (in Japanese)

Kono, Y., Manabe, K., Sato, K., and Sato, Y. 1998. Study on characteristics of pipe material of dynamic pipe fracture by waterhammer. *Annual Journal of Hydraulic Engineering*, 42, 835-840. (in Japanese)

Kono, Y., and Watanabe, M. 2002. Occurrence of vaporization and negative wave pressure of waterhammer. *Advances in Hydraulics and Water Engineering: Proceedings of the 13th IAHR-APD Congress*, 1, 430-434. Singapore: World Scientific Publishing Company.

Kono, Y., Moriya, T., Yuri, S., and Watanabe, M. 2005. Water hammer study in pipe network. *Proceedings of International Conference on Modeling Tools for Environmental and Resources Management*, 569-578. Bangkok: Asian Institute of Technology.

Narisawa, I. 1982. *The Strength Study of High Polymer Materials*. Tokyo: Ohomu Book Company. (in Japanese)

Watters, G. Z. 1979. *Modern Analysis and Control of Unsteady Flow in Pipelines*. Ann Arbor: Ann Arbor Science Publishers.

Wylie, E. B., and Streeter, V. L. 1978. *Fluid Transients*. New York: McGraw-Hill International Book Company.